(This is a sample cover image for this issue. The actual cover is not yet available at this time.)

A new physical model based on cascading column experiments to reproduce the radial flow and transport of micro-iron particles

Silvia Comba *, Jürgen Braun

University of Stuttgart, VEGAS - Research Facility for Subsurface Remediation, Stuttgart, Germany

ARTICLE INFO

ABSTRACT

In the field of aquifer restoration and civil engineering, fluids and suspensions are delivered in porous media via well injection. The flow field resulting around the well is three-dimensional. Since two and three-dimensional experiments which can be used to reproduce such flow fields are, although accurate, extremely elaborate and time consuming, the authors suggest to substitute them by a cascade of interdependent, one-dimensional (column) experiments. The new method is used to simulate the injection in aquifers of micro-iron particles dispersed in a shear thinning gel of guar gum and allows the prediction of iron particle distribution around the well and of injection pressure. The method respects the mass balance at the field scale and its predictions are in good agreement with those of a mathematical model proposed in the literature.

The method is consistent with the Triad Approach, a way to improve remediation efficiency proposed by the U.S. Environmental Protection Agency. The representativeness of the proposed tests combined with their simplicity and relative inexpensiveness make this new method applicable and useful in the planning and design of real remediation.

© 2012 Published by Elsevier B.V.

1. Introduction

Zero-valent iron particles in permeable reactive barriers (PRB) can be used to effectively remove groundwater contaminations from an aquifer (Gillham and O'Hannessin, 1994). However, PRB require a high initial investment which increases with depths. Moreover, they cannot be installed underneath buildings. To overcome these obstacles it has been suggested to inject iron particles with dimensions ranging from tens of nanometers to some micrometers (Zhang, 2003). The main advantages of these particles are that they are very reactive due to their large specific surface area, they can be applied directly into a source zone, and they can be injected via wells to remediate the soil under buildings,

with little or no reduction in building functionality. Field application of such particles has been documented at more than 100 sites around the word (Comba et al., 2011b; Müller et al., 2011)

To be injected, iron particles are dispersed in a carrier fluid which can be either a gas, an aerosol or a liquid. In this work the fluid phase is a liquid, which together with iron particles forms a slurry or a colloidal suspension. Injection is advantageous with respect to economy and invasivity, provided that iron particles are effectively delivered to the contaminants to ensure proximity to the contaminant, and hence chemical reactions (Illinois Environmental Protection Agency, 2001).

After a successful injection in a homogeneous porous medium, the zone saturated by the slurry has roughly the shape of a cylinder with height H depending on the length of the screened well section and on the soil stratification (or bedding) and with radius ROI or radius of influence depending on the injected volume, on soil porosity, and on H. Depending on the volume to be treated and site-specific

* Corresponding author.
E-mail addresses: slv.comba@gmail.com (S. Comba),
juergen.braun@iws.uni-stuttgart.de (J. Braun).

parameters, several vertically or horizontally overlapping injections may be necessary. Failure to obtain such an effective distribution of the reagents in the treatment zone results in pockets of untreated contaminants. This will reduce the effectiveness of the remediation. It can also happen that the existence of untreated zones is discovered months after the injection by observing contaminant concentration rebound. This could entail injection repetition with consequent negative effects on costs and site availability. Cases where the outcome did not meet expectations due to a bad distribution of iron particles are reported by Gavaskar and Condit (2005) and by Henn and Waddill (2006).

To effectively distribute iron particles via injection two conditions are to be warranted: (i) the liquid phase has to reach and contact the target area, and (ii) the liquid phase needs to be capable of carrying the solid particles sufficiently long to ensure delivery. The first condition concerns many applications besides the use of iron particles for aquifer remediation: in civil engineering various chemical solutions are delivered into porous media to seal or improve the mechanical resistance of soils; in aquifer restoration mixtures of surfactants and solvents are used to mobilize and recover oil or solvent phase; in reservoir engineering polymeric solutions enhance the recovery of oil from the oil bearing strata. The phenomenon depends both on the soil and on the liquid properties. The second condition concerns only the injection of colloidal suspensions, like iron slurries or cementitious grouts. It is basically a reverse application of the filtration laws since conditions with the least filtration efficiency allow for maximum particle transport. The condition is hard to satisfy when using iron particles, since the high density of iron results in rapid particle sedimentation in porous media (Phenrat et al., 2007; Tiraferri et al., 2008). Also the tendency of iron particles to aggregate in large clusters determines their accumulation in porous media, as it further increases particle sedimentation and as it determines the phenomenon of ripening (Elimelech et al., 1998).

A viscosity increase of the liquid phase is beneficial to satisfy both conditions, since it reduces fingering of the injected suspension and stabilizes the injection front (Martel et al., 1998, 2004: Zhong et al., 2008). It also decreases the aggregation of the iron particles while increasing their sedimentation time (Comba and Sethi, 2009). The viscosity increase can be achieved using special polymers with shear thinning properties such as guar gum or xanthan gum (Cantrell et al., 1997a, 1997b; Comba and Sethi, 2009; Comba et al., 2011a; Dalla Vecchia et al., 2009; Oostrom et al., 2007).

Another major factor controlling colloidal transport is the flow (seepage) velocity of the liquid phase. In order to satisfy continuity, flow velocity decreases hyperbolically with distance from an injection well. According to filtration theory, such a decrease in seepage velocity results in a reduction of particle mobility or an increase of the fraction of iron particles lost from the slurry and deposited in inter-granular voids. When using shear thinning fluids, the velocity decrease around the well has the additional effect of reducing the shear rate, which causes an increase in the apparent viscosity of the liquid phase. This increase in viscosity may retard colloidal particle sedimentation, and thus decrease the fraction of iron particles lost from the slurry and deposited in the porous medium.

In addition, at the field scale, synergistic effects between the abovementioned factors can occur (as all phenomena occur simultaneously at the large scale). Site-specific and secondarily phenomena are also likely to appear (as an example the degradation of guar gum in real injection conditions, with variable injection time from preparation and temperature; Comba and Braun, 2012)

To predict iron distribution around a well, the transport behaviour is usually attributed to a number of physical mechanisms taking place at the microscopic level, and to their interdependencies. Among these mechanisms are sedimentation (Rajagopalan and Tien, 1976; Tufenkji and Elimelech, 2004; Yao et al., 1971), interception (Rajagopalan and Tien, 1976; Tufenkji and Elimelech, 2004; Yao et al., 1971), Brownian diffusion (Rajagopalan and Tien, 1976; Tufenkji and Elimelech, 2004; Yao et al., 1971), surface attachment (Elimelech, 1993), ripening (Darby and Lawler, 1990; Tobiason, 1989; Tobiason and Vigneswaran, 1994), blocking (Hunt et al., 1993; Johnson and Elimelech, 1995; Ko and Elimelech, 2000), straining (McDowell-Boyer et al. 1986, Bradford et al., 2006a, 2006b), and hydrodynamic bridging (Ramachandran and Fogler, 1999). Sedimentation or retention of the particles is also influenced by surface roughness of soil particles (Kretzschmar et al., 1997; Redman et al., 2001), charge heterogeneity (Johnson and Elimelech, 1995), and variability in colloid characteristics (Bolster et al., 1999). To find these dependencies, colloidal transport tests in columns filled with porous medium are performed and constitutive relations are derived therefrom. However, as the number of relevant physical mechanisms increases, it becomes difficult to isolate the effect of each mechanism in the results of column tests.

Another approach that predicts iron micro-particle distribution around a well based on empirical mathematical modeling was adopted by Comba and Braun (2012). For this approach column tests are also performed and interpreted based on the main mechanisms proposed by colloid filtration theory. However, this approach is not based on constitutive relations derived from phenomena occurring at the micro scale, but is an empirical mathematical relationship that links transport behaviour to field variables (such as injection rate or volume of slurry injected).

The large number and the complexity of the phenomena described above suggest that prior to a field application it is necessary to verify the prediction of iron distribution generated by the mathematical models with laboratory experiments. Such experiments should reproduce as closely as possible the real flow situation expected during a field application. Ideally, porous medium extracted from the concerned zone should be used. Also, the guar gum utilized should come from the same supplier and should be prepared as in the field. In this way all phenomena and interactions influencing transport will be taken in account, including the ones not yet well known or unexpected for the specific conditions.

Currently, the only way to reproduce radial flow is to conduct three-dimensional or at least two-dimensional, radially symmetrical, experiments (Chao et al., 2000; Kobus et al., 1995; Müller and Nowack, 2010). Since these physical models are extremely elaborate and time consuming, the authors suggest substituting them by a cascade of interdependent, one-dimensional (column) experiments. This cascading column method is applied to the injection of micro-iron particles dispersed in a shear thinning gel of guar gum into aquifers. The method is used to select suitable injection parameters (flow
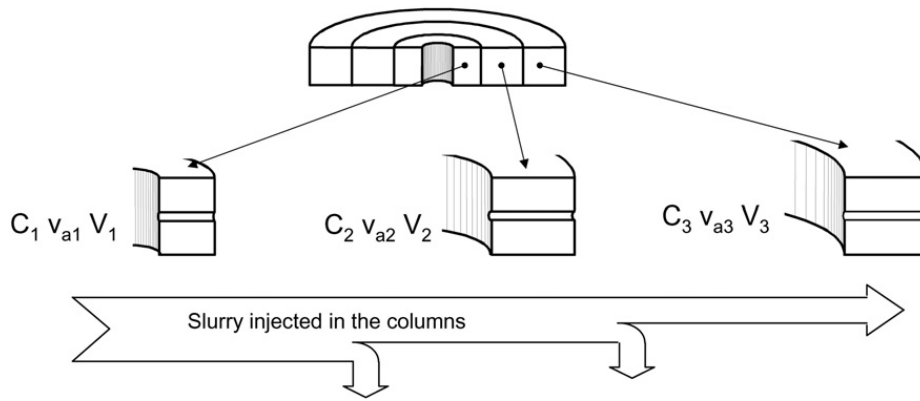
Fig. 1. Scheme of 3D column method.

rate of the field pump, ROI, guar gum concentration, etc.) for a given soil. Results are also compared to iron distribution obtained through a mathematical model proposed by Comba and Braun (2012). General indications about the purpose for which the method should be used are given. The method is simple, low cost, fast and able to immediately provide results without further elaborations. Due to these characteristics, the method is coherent with the Triad Approach proposed by US EPA (Interstate Technology and Regulatory Council, 2003), which aims at improving the remediation efficiency through the use of real-time technologies. This approach "acknowledges that environmental media are fundamentally heterogeneous at both larger and smaller scales"; therefore, it attaches great importance to the representativeness of the data. In fact, if the site is heterogeneous, the traditional way to characterize it (few samples analyzed with high accuracy) may create a false picture due to the risk that sample is not representative of what the data user thinks it represents. This risk is reduced by increasing the number of samples and analyzing them with methods having a lower accuracy (high-analytical quality in analysing single samples is seldom required) and, moreover, in evaluating their representativeness through the Conceptual Site Model (CSM). At this point, if required, characterization can be perfected by high-analytical quality analysis of few samples whose representativeness is ensured by the previous high-density sampling.

2. Theory/calculation section: Cascading columns and theory of dimension transformation

It is proposed to study the coupled problem of flow and colloidal transport in radial flow by discretizing the volume going from the well to the Radius of Injection or ROI (i.e. the distance from the well travelled by a fluid during the injection time neglecting diffusion and dispersion) in 3, 5 or 7 ideal concentric shells, each of which is characterized by a velocity value, by a volume of injected slurry and by the corresponding duration of flow of slurry in the respective shell. The flow in each shell is reproduced with a 1D column having the length equal to the thickness of the corresponding shell and the average parameters (seepage velocity and volume of slurry that flows through a unit surface perpendicular to the slurry flow) of the shell. A fraction of the slurry discharged from each column is re-injected in the next column in order to reproduce the concentration decay across the shell. The typical result of a test is iron concentration as a function of the distance from the well, which results from putting the concentration profile obtained for subsequent column tests side by side (see as an example Fig. 3). The method also allows an estimation of injection pressure, as a sum of the pressure drops recorded for each column of a set. A scheme of the method – that has been called the "3D column method" or "cascading column method" – is shown in Fig. 1.
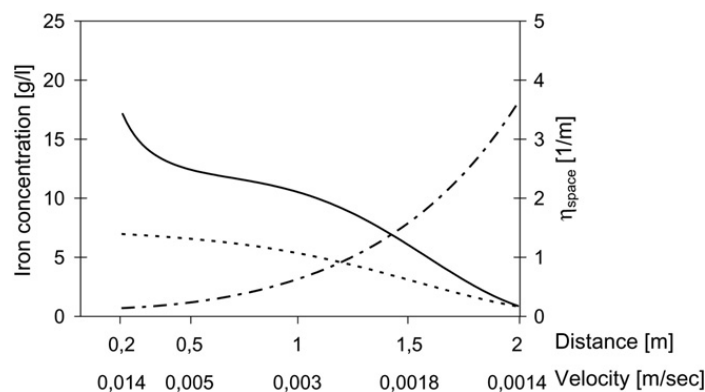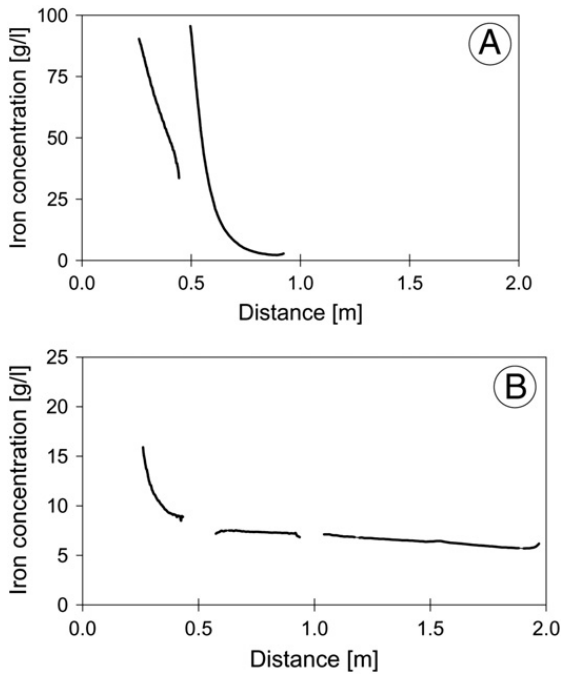

Fig. 2. Mathematical model prediction as a function of the distance from the injection well: deposition coefficient (dash dotted line), iron concentration in the slurry (dotted line) and iron concentration retained in the porous medium voids (continuous line).

Fig. 3. Results of the first experimental part. (A) (Left) Iron distribution around the injection well obtained using a slurry with 3 g/l guar gum and 7 g/l iron concentration and discretizing the flow domain with 3 columns of equal length. The total injection pressure is 3 bar. (B) (Right) Iron distribution around the injection well obtained using a slurry with 6 g/l guar gum and 7 g/l iron concentration and discretizing the flow domain with 3 columns of equal length. The total injection pressure is 4 bar.

Dimensioning of the method is as follows.

In a radial flow field velocity decreases by $1/r$ with increasing distance r from the injection point:

$$q = \frac{Q}{A} = \frac{Q}{2\pi m r} \tag{1}$$

where q is the Darcy velocity [LT^{-1}], Q is the total discharge [L^{3}T^{-1}], A is the area perpendicular to flow, r is the distance from the injection point [L] and m is the thickness of the aquifer [L].

The average velocity in each concentric section, and consequently the velocity in the corresponding column, can be calculated as the harmonic mean of the integrated continuity equation (Eq. (1)) over the domain. Using the harmonic mean, the travel time through a length equal to the section thickness will be exactly the real travel time.

The volume of slurry injected in each column is calculated as follows: the total volume $V_{\text{cross-area}}$ of slurry crossing a concentric cylindrical section of porous medium [L^3] as a function of the distance r from the well is:

$$
\begin{aligned}
V_{\text{cross-area}} &= \text{Volume that crosses the cylindrical area} = \\
&= \text{Volume}_{\text{ROI}} - \text{Volume}_r = \\
&= \left(\pi \cdot \text{ROI}^2 \cdot m \cdot \right) - \left(\pi \cdot r^2 \cdot m \cdot \varphi\right) = \\
&= \pi \cdot m \cdot n \cdot \left(\text{ROI}^2 - r^2\right)
\end{aligned} \tag{2}
$$

where Φ is the porosity.

The volume crossing a unit section $V_{\text{cross-unit-area}}$ of porous medium [L^2] as a function of the distance r is therefore:

$$
\begin{aligned}
V_{\text{cross-unit-area}} &= \frac{V_{\text{cross-area}}}{A \cdot \varphi} = \\
&= \frac{\pi \cdot m \cdot \varphi \cdot \left(\text{ROI}^2 - r^2\right)}{2 \cdot \pi \cdot m \cdot r \cdot \varphi} = \\
&= \frac{\text{ROI}^2 - r^2}{2r}
\end{aligned} \tag{3}
$$

The average volume per area in each concentric section $\overline{V_{\text{cross-unit-area}}}$ [L^2] is calculated as the arithmetic mean of the integrated Eq. (3) over the domain. The volume of suspension that should be injected in the column can thus be obtained by multiplying $\overline{V_{\text{cross-unit-area}}}$ by the effective cross sectional area of the column.

The duration of the column injection can be calculated as:

$$t = t_{\text{ROI}} - \frac{V_{\text{cross-area}}}{Q} \tag{4}$$

where t_{ROI} is the total duration of the injection at a given flow rate Q.

Finalizing the coupling between the 2D and the 1D problem consists of assigning to each column the corresponding parameters of the radial flow. If the column length was infinitesimal there would be no approximation.

Tests are performed by dividing the distance from the well to the ROI in different numbers of concentric shells (3–5–7). The following two criteria are employed to find the best trade-off between simplicity and accuracy:

- the thickness of each section is constant thus

$$L = \frac{\text{ROI} - \text{GCR}}{n} \tag{5}$$

where L is the section thickness [L], n is the total number of sections (number of subdivisions of the discretized domain) and GCR is the radius of the central cylinder including the well and its proximity (called "gray cylinder") [L]. The "gray cylinder" zone is not reproduced in the experiments since the high velocities of the slurry in this zone minimize particle sedimentation and determine phenomena like soil fracturing or its fluidification, which would be difficult to reproduce. Moreover, in this zone the slurry exiting the well screen is not yet uniformly distributed in the porous medium, but concentrated in the direction of the pipe holes.

- The average velocity over each section maintains the same ratio to the velocity of the next section (continuity), thus

$$\bar{q}_{i+1} = \alpha \cdot \bar{q}_i \tag{6}$$

With this method, the section thickness increases going from the injection point to the ROI.

The experiments reproduce a full radial flow field having the geometry and boundary conditions presented in Table 1 and in Fig. S2. Such parameters are based on realistic field injections to ensure transferability of the result to field situations.

Table 1
Geometry and boundary conditions for the full radial flow reproduced by the cascading column experiments.

|	
Radius of influence (m)	2
Gray cylinder radius (GCR) (m)	0.05
Screening length (m)	0.6

3. Materials and methods

3.1. Materials

Microscale zero-valent iron was provided by BASF, in form of carbonyl iron powder, commercially known as BASF-SM micro. According to the producer, the Fe content of the material is greater than 99%, while the particle diameters are below 10×10^{-6} m $(d_{10\%} = 2.1 \times 10^{-6}$ m, $d_{50\%} = 3.5 \times 10^{-6}$ m, $d_{90\%} = 5.5 \times 10^{-6}$ m).

Guar gum was purchased from Sigma Aldrich, in the form of a powder. Guar gum solutions with 2, 4 and 6 g/l guar gum concentrations are prepared by dispersing the required amount of solid polymer in deionized water and by thereafter subjecting the system to stirring. The suspensions are then filtered at 5×10^{-6} m to eliminate colloidal matter present in guar gum, which would plug the porous medium.

Micro-iron guar gum dispersions are prepared by adding the iron powder to the guar gum solution to reach an iron concentration of 7 g/l and by mixing the resulting suspension using a high shear rotor-stator processor for a total mixing time of 15 min for 8 l of suspension.

3.2. Column experiments

The experiments consist of columns packed with Silica sand (95% SiO_2) characterized by a grain size distribution
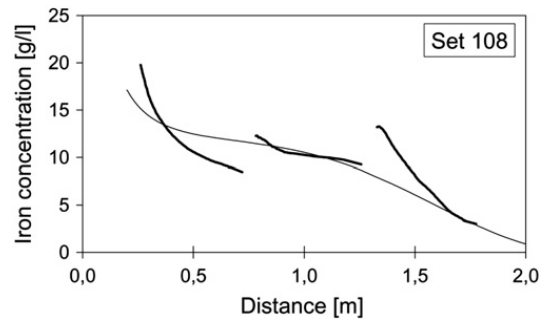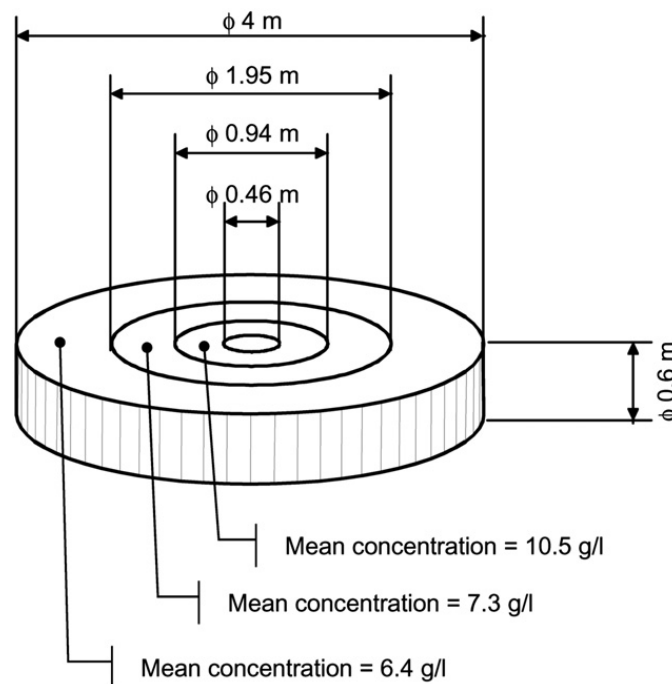

Fig. 5. Result of cascading column experiments using injection conditions specified in Materials and methods and a discretization of 3 columns of equal length (thick lines) and mathematical model prediction according to Comba and Braun (2012) (thin line).

between 0.6 and 1.2 mm. The columns are dry packed to an average total porosity of 36%, then flushed with CO_2 before being fully saturated with degassed water. The average hydraulic conductivity is 1.1×10^{-3} m/s, with a corresponding permeability of 1×10^{-10} m^2. The prepared columns are horizontally oriented and iron slurry is injected using a peristaltic pump, discharging the iron solutions at specified flow rates. The iron in the reservoir is kept suspended by a mixer. In each column experiment, the iron concentration in the column at the end of the test and the pressure drop across the column are measured.

3.3. Measurement of iron particles in the porous medium

The concentration of iron within the column is measured by a commercially available metal detector, which runs along the length of the column on a track and measures the electromagnetic inductance (Buchau et al., 2010; de Boer, 2007). To obtain the iron concentration from the metal detector output, the
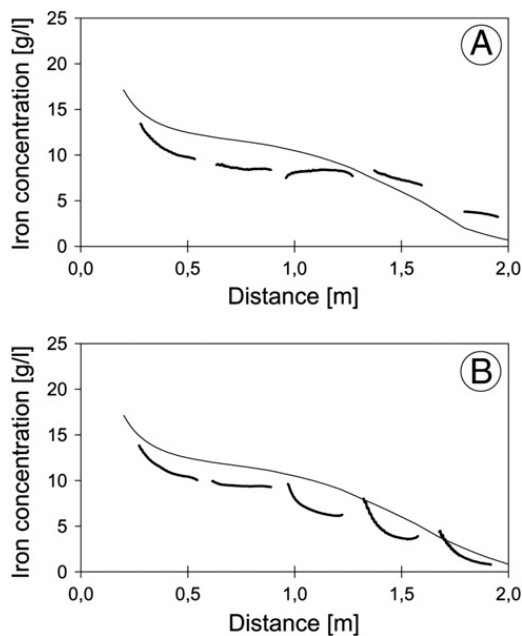

Fig. 4. Model cylindrical domain discretized into 3 shells following the criterion $\bar{q}_{i+1}/\bar{q}_i = const$. The results of the cascading column tests reported in Fig. 3 are reported for each shell in terms of average concentration of iron particles measured in each column.
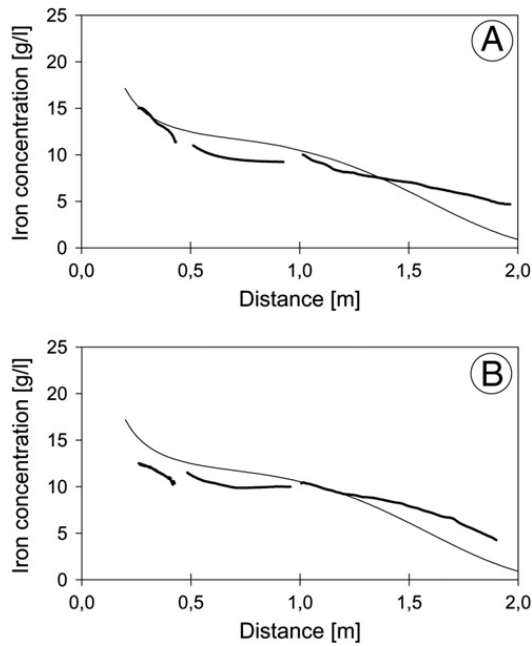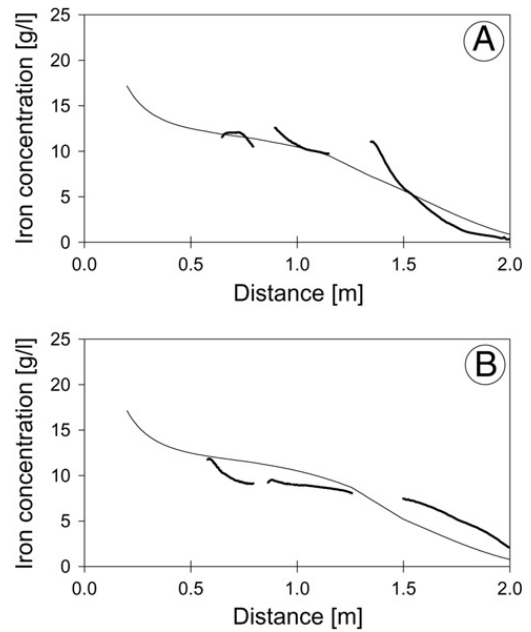
Fig. 6. Result (left, A) and replicate (right, B) of cascading column experiments using injection conditions specified in Materials and methods and a discretization of 3 columns of different length (thick lines). The mathematical model prediction according to Comba and Braun (2012) (thin line) is also reported.

Fig. 8. Result (left, A) and replicate (right, B) of cascading column experiments using injection conditions specified in Materials and methods and a discretization of 5 columns of different length (thick lines). Two columns reproducing the region near the well are excluded from the analysis due to their short length. The mathematical model prediction according to Comba and Braun (2012) (thin line) is also reported.

instrument has been calibrated by measuring a mixture of porous medium and various amounts of iron powder. The metal detector readings can be converted in the mass of iron along the column by subtracting the blank scan of the column filled with sand from the subsequent scan recordings during the injection, and correcting this signal using above mentioned calibration relation.

Because the metal detector is influenced by a region of porous medium rather than by a single point inside its coil, an incorrect signal is produced at the beginning and end of the test column, since in those regions the column cap is also detected. The effect of the boundary can be excluded by neglecting the initial and final 5 cm of the profile. In short columns, however, this may correspond to the loss of the entire profile. Therefore, columns having a length less than 20 cm value are excluded from the analysis. This is the case for the shortest columns representing the region near the well in Figs. 8 and 9. This failure in measuring iron content in one or more columns does not imply the failure of the whole experiment, since the slurry has been correctly filtered by the porous medium in the column and can be correctly injected into the following one. Therefore, the absence of results for one or two columns only implies a lack of knowledge about
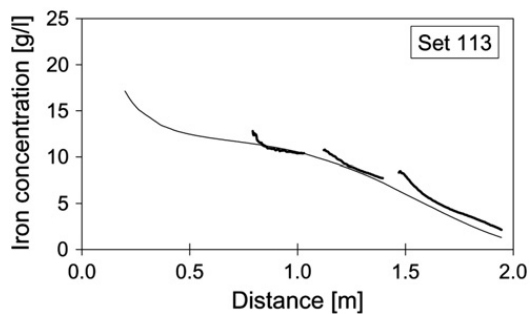

Fig. 7. Result (left, A) and replicate (right, B) of cascading column experiments using injection conditions specified in Materials and methods and a discretization of 5 columns of equal length (thick lines). The mathematical model prediction according to Comba and Braun (2012) (thin line) is also reported.

Fig. 9. Result of cascading column experiments using injection conditions specified in Materials and methods and a discretization of 7 columns of different length (thick lines) and mathematical model prediction according to Comba and Braun (2012) (thin line). Four columns reproducing the region near the well are excluded from the analysis due to their short length.

iron content in that zone, which normally extends only over few tens of centimetres.

3.4. Measurement of iron particles in the liquid phase

Iron concentration in the inflowing and outflowing slurry is measured through chemical analysis using the hydrogen evolution method. Two 100 ml headspace samples are taken from the inflow and outflow containers and analyzed for H_2 after adding a known amount of HCl. The method is based on the measurement of hydrogen forming due to chemical reaction of zero-valent iron and an acid (HCl); the volume of hydrogen is directly proportional to the amount of zero-valent iron material. The method has been calibrated by measuring weighted amounts of iron particles (as they are made of 99% zero-valent iron) using an analytical balance (Sartorius BP210S). Additional tests have been conducted to evaluate the kinetics of oxidation of iron particles, in order to evaluate whether the Fe^0 content of the particles varies during the tests and from the end of the test to the chemical analysis. According to the results, iron particles in guar gum solution do not change the Fe^0 content within 2 days. To conclude, through the hydrogen evolution method an accurate estimate of the mass of iron particles in guar gum suspension can be obtained.

Mass balance between iron concentrations in the inflow and outflow allows for calculations of the mass of iron within the column to confirm the accuracy and the calibration of the metal detector.

3.5. Pressure measurement

The pressure drop along the column is monitored by means of one pressure transducer that measures relative pressure.

3.6. Experimental design

In the first part of this study the cascading column method is applied to simulate a field operation. The goal is to experimentally determine radial transport distances for iron particles based on given initial and boundary conditions, and injection parameters (guar gum concentration and flow rate). Various experiments are performed, each with sets of 3 columns. The guar gum concentrations in the experiments are varied and a flow rate simulating injection conditions in an aquifer was applied.

In the second part of this study experiments to test discretization schemes are conducted with sets of 3, 5 and 7 columns having equal (Eq. (5)) or variable length (Eq. (6)). The range from 3 to 5 columns is the most interesting with respect to cost and simplicity of use; for this reason it was more deeply investigated. The parameters for the column sets are calculated as described previously in the section "Cascading columns and theory of dimension transformation." Replications are also performed. In this part of the study a suspension with 4 g/l guar gum and 7 g/l iron is used. The flow rate applied is based on the assumption that in the field an injection with a flow rate of 0.0037 m^3/s is applied and the screened length of the injection well is 0.6 m. Experimental conditions for each experiment are reported in Table S1.

3.7. Mathematical model

The results of the cascading column method are compared to the prediction of a numerical model which gives iron particle distribution around the injection well (Comba and Braun, 2012).

This mathematical model is an empirical mathematical relationship that links transport behaviour to field variables (such as injection rate, volume of slurry injected, etc.) and is based on a large number of column experiments. The model has been developed (and hence is valid) for specific initial conditions (porous medium and iron particle type, iron and guar gum concentration, packing mode of the porous medium, etc.), which are exactly the ones used in this study for the cascading column tests.

The mathematical model is based on the parameter "space removal efficiency" (η_{space}). Space removal efficiency is defined as the fraction of particle concentration lost by the slurry (and retained by the porous medium) while it crosses a unit length of the porous medium. Therefore, the smaller η_{space}, the more mobile are the iron particles. The relation between η_{space} and field parameters was studied in a previous paper (Comba and Braun, 2012). η_{space} is independent of the volume of the injected slurry (or the injection time) and particle concentration. On the contrary η_{space} is inversely proportional to seepage velocity (Fig. S1), as it decreases greatly until it reaches the region 3×10^{-3} m/s to 2×10^{-3} m/s, while for higher seepage velocities it levels out. This indicates that the values of seepage velocity from 2×10^{-3} m/s to 3×10^{-3} m/s represents a threshold, below which velocity the slurry has only a very limited capability to carry iron particles. This range of velocity will be called in the paper "critical threshold."

The outputs of the mathematical model, hypothesizing the same injection conditions as in the second experimental part, are shown in Fig. 2.

For the field case described above, the critical velocity values are located at about 1–1.5 m from the well; hence in the region from 1 to 1.5 m to the ROI, η_{space} increases sharply and reaches very high values (4 m^{-1}) at the ROI.

The mobile and immobile iron particle concentration are also reported in Fig. 2. Immobile particles consist of iron particles lost from the slurry that accumulate in the porous medium. Hence, the final amount of iron deposited at a given distance r from the well is a function not only of the deposition rate at such distance, but also of the amount of slurry that crosses a unit surface area of an imaginary cylinder of radius r. The specific volume depends on the desired ROI, and therefore on the total volume injected. The specific volume of slurry decreases hyperbolically as a function of the distance from the well (since all the injected slurry has to pass through the zones near the well, while only a limited amount of slurry will reach the ROI). This would point to a higher accumulation of particles close to the well as compared to further away. The total iron concentration in the voids of the porous medium can be obtained at a certain distance from the well as the sum of iron in the mobile phase at that distance and the iron deposited by the slurry in that zone.

For a field application the distribution of iron particles obtained in Fig. 2 is not optimal, since the injected iron mass is not homogeneously distributed in the domain (17 g/l of iron at the well and only 2 g/l at the ROI). In addition, in the zone from

1 to 1.5 m to 2 m a higher variability in iron concentration is expected, as guar gum solutions (and hence their transport capability of iron particles) are, at lower shear rates like the ones occurring in this region, particularly sensitive to handling and preparation conditions and hence are affected by an inherent variability (Comba and Braun, 2012). The above-mentioned low and uncertain iron concentration at large distances from the well indicates that injection conditions should be optimized for the field application. However, these conditions are suitable to test the cascading column method in the worst condition and hence they are used in the second part of the work. On the other hand this choice implies that our experiments are affected by a higher variability.

4. Results and discussion

The first part of this work, which aimed at optimizing different injection parameters (flow rate of the field pump, ROI, guar gum concentration, etc.) for the given soil. Two experiments from this phase are reported in Fig. 3.

A trial is reported in Fig. 3a using an equivalent field pump flow rate of 0.0037 m^3/s and a guar gum concentration of 3 g/l. The other injection conditions (as an example the ROI) are specified in Materials and methods. According to these results, the combination of guar gum concentration and flow rate is insufficient to ensure iron particle distribution, as the slurry loses all iron particles in the first column and at the beginning of the second one. This result could also be visibly observed during the test because the slurry discharging from the second column was transparent, while the iron suspensions are normally dark grey. In such conditions the experiment with the third column would have been useless and was thus omitted.

In subsequent tests, the guar gum concentration was increased to 6 g/l, maintaining the same flow rate (Fig. 3b). Also in this case an unambiguous result can be obtained with a discretization in three columns only, as iron particles reach the target distance of 2 m with a concentration similar to the injected one (about 5 g/l) and the profile of iron concentration is flat. The flatness of the profiles suggests that the iron particle deposition rate is low.

The results of the cascading column experiments in Fig. 3b were then transferred to the cylindrical domain(Fig. 4) in order to predict a mass balance calculation at the field scale. The iron mass in the field in each cylindrical region is calculated by multiplying the average concentration of a column by the void volume of the corresponding concentric cylindrical section. The total iron mass in the field (the sum of the abovementioned iron in each shell) is compared to the total theoretical amount of injected iron. Based on the injection parameters of the theoretical field injection, we expect to inject in the whole

hollow cylinder having a ROI of 2 m, a GSR of 0.2 m and a height of 0.6 m, a total of about 18 kg of iron particles (Table 2).

The closure of the mass balance (the difference between the iron mass theoretically injected in the model cylindrical domain and the calculated iron mass in the model cylindrical at the end of the injection is below 4%) proves the capability of the cascading column method to accurately reproduce reality. Such a good result was somewhat predictable, considering that the only approximation in the cascading column method in reproducing the reality is the discretization of two parameters (seepage velocity and specific volume of slurry).

The closure of the mass balance in conjunction with the fact that both tests shown in Fig. 3 gave clear results suggests that a discretization in only 3 columns, even if the number of columns is rather low, can ensure sufficient accuracy and reliability in evaluating the distance travelled by iron particles and their subsequent distribution.

Besides iron distribution, the injection pressure should also be evaluated in order to choose a suitable pump and to assess the risk of daylighting, especially in case of injection close to the soil surface (Truex et al., 2011). As an example, the pressure recorded during the injection in the experiment depicted in Fig. 3b (set 103) is 4 bars (pressure is not displayed in the figure). If this value should be too high it must be reduced by reducing guar gum concentration and/or field pump flow rate. Such reduction(s) will cause an impairment in iron distribution as velocity will become closer to the critical threshold or even below (Fig. S1). The smoothness of the profile shown in Fig. 3b is a clear sign that the velocity is above the critical threshold. A more irregular and variable distribution necessitates an optimization of the discretization criterion. Such optimization is the scope of the second phase of this work.

In the second part of this work the discretization scheme is varied. The results are reported in Figs. 5–9. The experimental conditions are: guar gum concentration 4 g/l, iron concentration 7 g/l, an equivalent field pump flow rate of 0.0037 m^3/s and injection conditions as specified in Materials and methods. In each figure the prediction of iron concentration according to the model proposed in Comba and Braun (2012) is also reported. Iron concentration is the sum of the iron particles in the mobile phase and of immobile particles that have been retained by the porous medium. Based on the results shown in Figs. 5–9 a new parameter, the "useful radius," is introduced in Table 3. The "useful radius" is defined as the distance at which the total concentration in the porous medium is equal to half the concentration of the slurry injected into the first column (7 g/l), assuming that such concentration is the minimal acceptable in the field.

Discretization schemes can be chosen according to the following reasoning:

Table 2

First experimental part. Comparison between the mass of iron theoretically injected in the cylindrical domain and the mass of iron in the cylindrical domain at the end of the injection according to the results of the cascading column experiments.

Sorgente dei dati	Shell #	Inside diameter [m]	Outside diameter [m]	Volume (voids) [m^3]	Iron concentration [g/l]	Total iron [kg]
Experiments	1	0.46	0.94	0.108	10.5	1.1
	2	0.94	1.95	0.468	7.3	3.4
	3	1.95	4	1.954	6.4	12.5
					Total	17.1
Theoretical	Whole cylindrical domain	0.46	4	2.53	7	17.7

Table 3
Comparison of the experiments characterized by different discretization criteria based on the distance from the well where concentration is equal to half of the injected one.

# of columns	Discretization criterion	Set #	Useful radius [m]
3	$L = $ const	108	1.72
3	$\bar{q}_{i+1}/\bar{q}_i = $ const	104 (109)	>2 and >2
5	$L = $ const	112 (148)	1.9 and 1.7
5	$\bar{q}_{i+1}/\bar{q}_i = $ const	110 (111)	1.7 and 1.85
7	$\bar{q}_{i+1}/\bar{q}_i = $ const	113	1.78
	Model		1.72

The most interesting/important zone is the one farther from the injection well because the iron concentration in this zone determines the useful radius. Moreover, due the cylindrical shape of the flow domain, the volume decreases hyperbolically as a function of the distance. Therefore the iron concentration close to the injection well concerns only a small part of the field volume.

If, despite its minor importance, the iron concentration near the well is wanted, a finer discretization is necessary because close to the well the most influential factor, the specific volume, changes rapidly. If the first column is one third of the ROI length, the prediction for this zone is not very accurate (Fig. 5). The zone farther from the injection well on the other hand does not require necessarily a fine discretization. As an example it has been shown (Fig. 3b) that for some distance from the well, a column having a length equal to half the radius gives a good result. Instead, when (Fig. 6a and b) the slope of iron concentration profile is higher in a column compared to the previous one, it is likely that in such a zone seepage velocity is close to the critical range of velocity. In this case a finer discretization is necessary.

Some sets show inaccuracies such as the shift of contiguous profiles in the vertical direction. As an example in Fig. 7b, while the results of the first two columns form a continuous line, for the subsequent columns the iron concentration at the end of one column differ slightly from the one at the beginning of the subsequent one. These inaccuracies need to be put in perspective with respect to the total prediction. It is important to realize that the overall experiment is to reproduce reality in full-size scale. Therefore the observed inaccuracies are much less critical compared to traditional column tests. If the graphs are compared based on the distance at which a certain concentration occurs (rather than by comparing the concentrations at a certain distance) it can be shown that different experiments differ for a few tens of centimetres, as proved by the fact that in all these five sets the useful radius ranges from 1.7 to 1.9 m. Such a range of variability is negligible in a field application because when determining the distance between injection points, a suitable safety factor (partial overlapping of injection zones) should be used in any case to take into account the fact that the injected zone can not be a perfect cylinder uniformly filled all the way to its perimeter. In conclusion, although the discretization scheme changes, the results are in good agreement with each other. This result proves the capability of the method to work in different conditions. It shows a robustness, which is a fundamental requirement when real-time measurement is required.

Required pressure drop as a function of distance can be also estimated through the cascading column method, as done in Fig. 10, by adding to the pressure drop of a column, the sum of the pressure drops measured for the subsequent columns.

When displaying pressure data on a graph, each cumulative pressure value should be reported at the distance r where the corresponding shell begins. However, the experimental parameters of a shell (as an example seepage: velocity) are those of an internal point of the shell and hence are reduced compared to the ones at the column beginning (as an example: seepage velocity). Therefore a safety factor should be applied to the total injection pressure estimate to account for this difference.

The results for injection pressure obtained using different discretization criteria are in good agreement with each other (difference in the range of 10%) and indicate an injection pressure of about 2 bars (or hydraulic head of 20 m of water).

Experiments can be compared with modeling prediction for iron distribution (Comba and Braun, 2012). There is in general a very good agreement between the experiments and the iron distribution predicted by the mathematical model. Both show a monotonic decrease in iron concentration going from the well to the ROI and both predict similar iron concentrations. In addition, both show a central region (from approximately 0.7 m to 1.3 m) where iron concentration levels out.

The agreement between experiments and mathematical model verifies the distribution of iron around the well through the comparison of the shapes of the curves of iron concentration as a function of distance. Furthermore, it verifies the total mass of iron retained in the porous medium; in this case the mathematical model represents a sure reference because the mass balance is based upon geometrical calculations. The very good agreement between experiments and model further proves the effectiveness of both approaches.

Although the mathematical and the proposed physical models are in good agreement, we believe that their range of application differs. The mathematical model for predicting iron distribution has been developed based on a very large number of independent column tests so it is rather robust. Nevertheless, small differences in the real conditions compared to those of the model (e.g. slight differences in guar gum solution due to a delay in its use after the preparation) or the difficulty in estimating a model parameter could reduce the accuracy and the reliability of the results. On the other hand, trying to take into account in the model all the possible secondary conditions would be not only arduous, but it would reduce the reliability of the model due to the
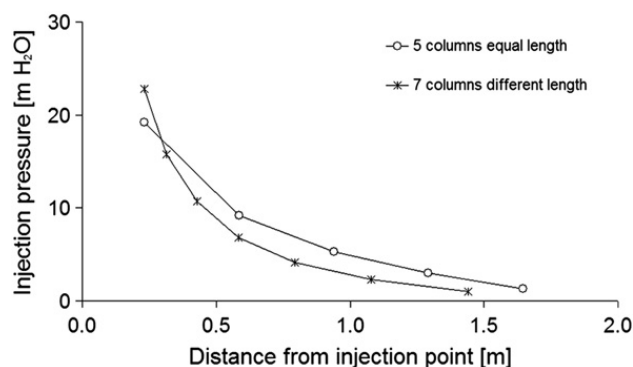
Fig. 10. Pressure field around the injection well obtained through 3D experiments (symbols) for 4 g/l guar gum and 7 g/l iron suspension injected at a flow rate of 0.0037 m^3/s obtained with two discretization criteria.

large number of influencing factors. The second method overcomes all these by reproducing specific field conditions. In conclusion, we suggest the following application of the two models to a practitioner in charge of designing a field application: to use the robust and experimental mathematical model to design the treatment, but then to take the final decisions using the quick, simple and inexpensive "3D-column" physical model.

The applicability and usefulness of the cascading column method in real remediation applications emerges when analyzing it following the criteria of the Triad Approach (Interstate Technology and Regulatory Council, 2003). The Triad Approach can be transferred to the testing of iron transport: instead of one or few high-accurate but not necessarily representative tests, the overall accuracy is much better ensured by multiple reasonably accurate tests repeated in zones of the site having different properties, in order to optimize slurry and injection parameters in each zone. Thanks to its simplicity (columns can be filled with porous medium extracted from the zones to be tested or with an equivalent one) and its limited cost, cascading column method makes this possible. The representativeness of the cascading column tests is very good because features such as mean soil properties, distance travelled by iron particles, seepage velocity, specific volume, and decay in slurry concentration along the travel from injection well to ROI are reproduced in full-size scale, while the only approximation is the discretization of the last three parameters.

Due to its characteristics of quickness and simplicity in execution and data interpretation, cascading column method is consistent with other characteristics of the Triad Approach; that is to use technologies "real time" to support a "dynamic work strategy," thus saving costs and reducing time losses.

5. Conclusions

In this paper a new method to simulate the fluid injection via wells is presented. The method consists in a cascade of interdependent column experiments. The main characteristics of the method are summarized below:

- The method provides iron particle concentration as a function of the distance from the well and injection pressure. In this way the method enables one to verify if the distance travelled by iron particles is sufficient, if iron particles are distributed with the desired uniformity within the domain and if the injection pressure is sufficiently low.
- The method respects the mass balance at the field scale.
- Since there exists a threshold for velocity below which the capability of the slurry to carry iron particles drops sharply, the cascading column method generally gives a good estimation with a discretization of three columns only. Nevertheless, when it is necessary to minimise pressure by working near that threshold a finer discretization may be appropriate.
- There is a very good agreement between the physical model and the mathematical model proposed in Comba and Braun (2012).
- The method is able to reproduce the specific field conditions, that would be arduous to describe through mathematical models.
- The cascading column method is complimentary to mathematical models. We suggest the following application of the two models to a practitioner in charge of designing a field application: to use the robust and experimental mathematical model (Comba and Braun, 2012) to design the treatment, but then to take the final decisions using the quick, simple and inexpensive "3D-column" physical model.
- The cascading column method is a fast, accurate and straightforward tool useful in decision making and consistent with the Triad Approach proposed by US EPA.

Acknowledgements

Appendix A. Supplementary data

Supplementary data to this article can be found online at http://dx.doi.org/10.1016/j.jconhyd.2012.07.003.

References

Bolster, C.H., Mills, A.L., Hornberger, G.M., Herman, J.S., 1999. Spatial distribution of deposited bacteria following miscible displacement experiments in intact cores. Water Resources Research 35, 1797–1807.

Bradford, S.A., Šimůnek, J., Bettahar, M., van Genuchten, M.Th., Yates, S.R., 2006a. Significance of straining in colloid deposition: evidence and implications. Water Resources Research 42.

Bradford, S.A., Šimůnek, J., Walker, S.L., 2006b. Transport and straining of E. coli O157:H7 in saturated porous media. Water Resources Research 42.

Buchau, A., Rucker, W.M., de Boer, C.V., Klaas, N., 2010. Inductive detection and concentration measurement of nano sized zero valent iron in the subsurface. IET Science, Measurement & Technology 6, 289–297.

Cantrell, K.J., Kaplan, D.I., Gilmore, T.J., 1997a. Injection of colloidal size particles of Fe0 in porous media with shear thinning fluids as a method to emplace a permeable reactive zone. Land Contamination and Reclamation 5, 253–257.

Cantrell, K.J., Kaplan, D.I., Gilmore, T.J., 1997b. Injection of colloidal Fe-0 particles in sand with shear-thinning fluids. Journal of Environmental Engineering-ASCE 123, 786–791.

Chao, H.-C., Rajaram, H., Illangasekare, T.H., 2000. Intermediate scale experiments and numerical simulations of transport under radial flow in two-dimensional heterogeneous porous medium. Water Research 36, 2869–2878.

Comba, S., Braun, J., 2012. An empirical model, developed from numerous 1D column experiments, to predict the distribution of iron micro-particles in a radial flow domain. Journal of Contaminant Hydrology 132, 1–11.

Comba, S., Sethi, R., 2009. Stabilization of highly concentrated suspensions of iron nanoparticles using shear-thinning gels of xanthan gum. Water Research 43, 3717–3726.

Comba, S., Dalmazzo, D., Santagata, E., Sethi, R., 2011a. Rheological characterization of xanthan suspensions of nanoscale iron for injection in porous media. Journal of Hazardous Materials 185, 598–605.

Comba, S., Di Molfetta, A., Sethi, R., 2011b. A comparison between field applications of nano-, micro-, and millimetric zero-valent iron for the remediation of contaminated aquifers. Water, Air, and Soil Pollution 215, 595–607.

Dalla Vecchia, E., Luna, M., Sethi, R., 2009. Transport in Porous Media of Highly Concentrated Iron Micro- and Nanoparticles in the Presence of Xanthan Gum. Environmental Science and Technology 43, 8942–8947.

Darby, J.L., Lawler, D.F., 1990. Ripening in depth filtration: effect of particle size on removal and head loss. Environmental Science and Technology 24, 1069–1079.

De Boer, C., 2007. Characteristics and Mobility of Zero-Valent Nano-Iron in Porous Media a Laboratory Assessment Study, MS thesis, Utrecht University.

Elimelech, M., 1993. Predicting collision efficiencies of colloidal particles in porous media. Water Research 26, 1–8.

Elimelech, M., Jia, X., Gregory, J., Williams, R., 1998. Particle Deposition & Aggregation: Measurement, Modelling and Simulation. Butterworth-Heinemann.

Gavaskar, A., Condit, W., 2005. Nanoscale Zero-Valent Iron Technologies For Source Remediation. US EPA Contract Report Cr-05-007-Env. Available at www.clu-in.org/download/remed/cr-05-007-env.pdf.

Gillham, R.W., O'Hannessin, S.F., 1994. Enhanced degradation of halogenated aliphatics by zero-valent iron. Ground Water 32, 958–967.

Henn, K.W., Waddill, D.W., 2006. Utilization of nanoscale zero-valent iron for source remediation - A case study. Remediation Journal 16, 57–77.

Hunt, J.R., Hwang, B.C., Mcdowellboyer, L.M., 1993. Solids accumulation during deep bed filtration. Environmental Science and Technology 27, 1099–1107.

Illinois Environmental Protection Agency, 2001. Leaking Underground Storage Tank Program: Use Of In-Situ Chemical Oxidant Compound Injection. Available at http://www.epa.state.il.us/land/lust/forms/technical-forms/chem-ox-design-guidance.pdf.

Interstate Technology and Regulatory Council (ITRC), 2003. Technical and Regulatory Guidance for the Triad Approach: A New Paradigm for Environmental Project Management (SCM-1) Available at http://www.itrcweb.org/SCM-1.pdf.

Johnson, P.R., Elimelech, M., 1995. Dynamics of colloid deposition in porous media: blocking based on random sequential adsorption. Langmuir 11, 801–812.

Ko, C.-H., Elimelech, M., 2000. The shadow effect in colloid transport and deposition dynamics in granular porous media: measurements and mechanisms. Environmental Science and Technology 34, 3681–3689.

Kobus, H., Barczewski, B., Koschitzky, H.P., 1995. Role of controlled experiments for research on groundwater contamination and remediation. International Journal of Rock Mechanics and Mining 32, 431–438.

Kretzschmar, R., Barmettler, K., Grolimund, D., Yan, Y.D., Borkovec, M., Sticher, H., 1997. Experimental determination of colloid deposition rates and collision efficiencies in natural porous media. Water Resources Research 33, 1129–1137.

Martel, K.E., Martel, R., Gelinas, P.J., 1998. Laboratory study of polymer solutions used for mobility control during in situ NDEL recovery. Ground Water Monitoring and Remediation 25, 103–113.

Martel, R., Hebert, A., Lefebvrea, R., Gelinas, P., Gabriel, U., 2004. Displacement and sweep efficiencies in a DNDEL recovery test using micellar and polymer solutions injected in a five-spot pattern. Journal of Contaminant Hydrology 75, 1–29.

McDowell-Boyer, L.M., Hunt, J.R., Sitar, N., 1986. Particle transport through porous media. Water Resources Research 22, 1901–1921.

Müller, N.C., Nowack, B., 2010. Observatory NANO focus report 2010 Nano zero valent iron – THE solution for water and soil remediation? Available at www.observatorynano.eu.

Müller, N.C., Braun, J., Bruns, J., Černík, M., Rissing, P., Rickerby, D., Nowack, B., 2011. Application of nanoscale zero valent iron (NZVI) for groundwater remediation in Europe. Environmental Science and Pollution Research 19, 550–558.

Oostrom, M., Wietsma, T.W., Covert, M.A., Vermeul, V.R., 2007. Zero-valent iron emplacement in permeable porous media using polymer additions. Ground Water Monitoring and Remediation 27, 122–130.

Phenrat, T., Saleh, N., Sirk, K., Tilton, R.D., Lowry, G.V., 2007. Aggregation and sedimentation of aqueous nanoscale zerovalent iron dispersions. Environmental Science and Technology 41, 284–290.

Rajagopalan, R., Tien, C., 1976. Trajectory analysis of deep-bed filtration with sphere-in-cell porous-media model. AICHE Journal 22, 523–533.

Ramachandran, V., Fogler, H.S., 1999. Plugging by hydrodynamic bridging during flow of stable colloidal particles within cylindrical pores. Journal of Fluid Mechanics 385, 129–156.

Redman, J.A., Grant, S.B., Olson, T.M., Estes, M.K., 2001. Pathogen filtration, heterogeneity, and the potable reuse of wastewater Environ. Particulate Science and Technology 35, 1798–1805.

Tiraferri, A., Chen, K.L., Sethi, R., Elimelech, M., 2008. Reduced aggregation and sedimentation of zero-valent iron nanoparticles in the presence of guar gum. Journal of Colloid and Interface Science 324, 71–79.

Tobiason, J.E., 1989. Chemical effects on the deposition of non-Brownian particles. Colloids and Surfaces 39, 53–77.

Tobiason, J.E., Vigneswaran, B., 1994. Evaluation of a modified-model for deep bed filtration. Water Research 28, 335–342.

Truex, M.J., Vermeul, V.R., Mendoza, D.P., Fritz, B.G., Mackley, R.D., Oostrom, M., Wietsma, T.W., Macbeth, T., 2011. Injection of zero valent iron into an unconfined aquifer using shear-thinning fluids. Ground Water Monitoring and Remediation 3, 50–58.

Tufenkji, N., Elimelech, M., 2004. Correlation equation for predicting single-collector efficiency in physicochemical filtration in saturated porous media. Environmental Science and Technology 38, 529–536.

Yao, K.M., Habibian, M.M., Omelia, C.R., 1971. Water and waste water filtration. Concepts and applications. Environmental Science and Technology 5, 1105–1112.

Zhang, W., 2003. Nanoscale iron particles for environmental remediation: an overview. Journal of Nanoparticle Research 5, 323–332.

Zhong, L., Oostroma, M., Wietsma, T.W., Covert, M.A., 2008. Enhanced remedial amendment delivery through fluid viscosity modifications: experiments and numerical simulations. Journal of Contaminant Hydrology 101, 29–41.